

Heavy flavor contributions to the Drell-Yan cross section

P.J. Rijken and W.L. van Neerven

Instituut Lorentz
 University of Leiden
 P.O. Box 9506
 2300 RA Leiden
 The Netherlands

January 1995

Abstract

We investigate the effect of heavy flavor contributions to vector boson ($V = \gamma, Z, W$) production which is described by the Drell-Yan mechanism. All reactions with bottom and top quarks ($Q_i = b, t$) in the final state, like $q_1 + q_2 \rightarrow V + Q_1 + Q_2$ and $g + g \rightarrow V + Q_1 + Q_2$, are considered. This study also includes the virtual contributions containing heavy flavor loops which were not taken into account earlier in the literature. Our analysis reveals that the above corrections to the Drell-Yan cross section are very small. Only at energies characteristic for the LHC they are of the same order of magnitude as the order α_s^2 QCD contributions due to light quark and gluon subprocesses calculated earlier in the literature.

1 Introduction

The production cross sections for the electroweak vector bosons W and Z in hadron-hadron collisions as described by the Drell-Yan (DY) [1] mechanism provides us with a beautiful test of perturbative QCD. One of the reasons is that the total cross section can be calculated in next-to-next-to leading order in perturbative QCD [2, 3] a result which is very hard to achieve for other processes in hadron-hadron collisions.

Another advantage of this process is that on the Born level it is purely electroweak in origin for which the theory is in an excellent shape. Hence each deviation of the cross section from the Born approximation can be attributed to QCD effects. Therefore the Drell-Yan (DY) process belongs to the same class as deep inelastic lepton hadron scattering and electron-positron collisions where QCD corrections can be measured with much higher accuracy than in other reactions.

Besides the total cross section for vector boson production and the cross section $d\sigma/dm$ where m denotes the lepton pair invariant mass order α_s^2 corrections due to soft plus virtual gluon contributions have been calculated in [4] to the differential distributions $d^2\sigma/dm dx_F$ and $d^2\sigma/dm dy$. Here the quantities x_F and y denote the fraction of the longitudinal momentum of the lepton pair with respect to the center of mass (CM) momentum and the rapidity respectively.

Furthermore one has computed the full order α_s correction to the single vector boson inclusive cross sections $d^3\sigma/dm dx_F dp_T$ or $d^3\sigma/dm dy dp_T$ [7] where p_T denotes the transverse momentum of the vector boson. All the above calculations have been performed under the assumption that the quarks, appearing in the partonic subprocesses contributing to the DY process, are massless. This is a reasonable assumption for the light quarks $u, d,$ and s and even for c since the masses of the W and Z are large compared with the masses of the above quarks. However this assumption is doubtful for the bottom quark and it is certainly wrong for the top quark since recent experiments [9] indicate that $m_t > M_W, M_Z$. Therefore we cannot neglect the masses of the bottom and top in the final state of the partonic subprocesses in particular if the collider CM energy is small like in the case of the SppS ($\sqrt{s} = 0.63 \text{ TeV}$) or the TEVATRON ($\sqrt{s} = 1.8 \text{ TeV}$). Maybe for some partonic subprocesses one can apply the zero mass approximation for the bottom quark at LHC ($\sqrt{s} = 16 \text{ TeV}$) as we will show later on. Contrary to the final state we will omit the bottom and top quarks in the initial state because we assume that the bottom and top densities in the hadron are negligibly small.

The calculation of the contribution of heavy flavors to the DY cross section has been performed for Z -production in [10]. It contained all one-loop and two-loop corrections which are characteristic of Z -production but do not contribute to W -production or processes with a photon in the intermediate state. They are characterized by the triangular heavy flavor-loop insertions containing the Adler-Bell-Jackiw anomaly which has to cancel while adding top and bottom loops. This work was extended in [11] by including the interference terms originating from the final and initial state radiation of the vector boson in the process $q + \bar{q} \rightarrow Z + Q + \bar{Q}$ (with $Q = b, t$). All other production mechanisms, which also show up for W -production and processes with a photon in the intermediate state, have not been considered yet. The contributions to

Z -production considered in [10, 11] all show up on the order $\frac{2}{s}$ level and amount to about 0.1 percent of the Born approximation which means that they are experimentally unobservable.

In this paper we want to complete the above analysis by including all remaining Feynman graphs which also contribute to lepton pair production with a W or a photon in the intermediate state. Apart of some additional two-loop graphs they contain the contribution of the partonic subprocesses $q_1 + q_2 \rightarrow V + Q_1 + Q_2$ and $g + g \rightarrow V + Q_1 + Q_2$ with $V = \gamma, Z, W$ and $Q_i = b, t$. Like the corrections discussed in [10, 11] they all contribute to the DY cross section on the order $\frac{2}{s}$ level.

This paper will be organized as follows. In section 2 we present the partonic cross sections corresponding to the subprocesses which contribute to heavy flavors plus vector boson production. Furthermore we show that in the case the vector boson mass becomes much larger than the heavy flavor mass one can find explicit analytic results. In section 3 we compute the heavy flavor contributions to vector boson production at current and future hadron-hadron colliders. In particular a comparison will be made between the order $\frac{2}{s}$ corrections due to light partons (quarks and gluons), calculated previously in [2, 3], and the contributions due to bottom and top quarks presented in this paper. Finally in Appendix A we give an explicit formula for the two-loop vertex correction which was not computed in [10, 11].

2 The order $\frac{2}{s}$ corrections to the DY cross section due to heavy flavor production

In this section we present the partonic cross sections of heavy flavor production contributing to the Drell-Yan (DY) process which is given by

$$H_1 + H_2 \rightarrow V + \text{"X"} \rightarrow \ell_1 + \ell_2, \quad (2.1)$$

where H_1, H_2 denote the incoming hadrons and V stands for one of the vector bosons of the standard electroweak model (γ, Z or W) which subsequently decays in the lepton pair ℓ_1, ℓ_2 .

The heavy flavors in the final state are given by Q_1 and Q_2 respectively and the symbol "X" denotes any inclusive final hadronic state. In lowest order of the electroweak and strong coupling constants the above reaction receives contributions of the following parton subprocesses

$$i(k_1) + j(k_2) \rightarrow V(q) + Q_1(p_1) + Q_2(p_2); \quad (2.2)$$

with $i, j = q, \bar{q}, g$. Here q stands for the light quarks given by u, d, s , and c whereas the heavy quarks are represented by t and b . Notice that in this paper we study heavy flavor production at large hadron collider energies so that the charm can be treated as a light quark whose mass can be neglected. In addition to reaction (2.2) we include the virtual corrections due to heavy flavor loops which contribute to the subprocesses

$$i(k_1) + j(k_2) \rightarrow V(q); \quad (2.3)$$

$$i(k_1) + j(k_2) \rightarrow V(q) + l(k_3); \quad (2.4)$$

with $l = q, \bar{q}, g$. The most of these virtual corrections reveal the presence of the triangle fermion loops giving rise to the well known Adler-Bell-Jackiw anomaly which has to cancel between the top and bottom contributions. They have been treated in [10, 11] in the case of $V = Z$. Here below we will add the contributions due to gluon self energies containing the heavy quark loop which also appear when V is represented by γ and W .

In the subsequent part of this paper we are interested in the following parton cross section

$$\frac{d\hat{\sigma}_{ij}^V}{dQ^2} = \hat{\sigma}_V(Q^2; M_V^2) \hat{W}_{ij}^V(\hat{s}; Q^2; m_1^2; m_2^2); \quad \hat{s} = \frac{Q^2}{s}; \quad (2.5)$$

receiving contributions from the reactions (2.2)-(2.4) ($i, j = q, \bar{q}, g$). The quantity $\hat{\sigma}_V$ represents the pointlike DY cross section and the kinematical variables \hat{s} ($\hat{s} = (k_1 + k_2)^2$) and $\frac{Q^2}{s}$ stand for the CM energy and the lepton pair invariant mass respectively. In addition to the above variables the DY structure function, denoted

by \hat{W}_{ij}^V , also depends on the heavy flavor masses m_1 and m_2 . The pointlike cross section refers to the reaction

$$q_1 + q_2 \rightarrow V \rightarrow \ell_1 + \ell_2; \quad (2.6)$$

and is given by (see [2, 3])

$$\sigma^V(Q^2) = \frac{1}{N} \frac{4}{3Q^4}; \quad (2.7)$$

$$\sigma_Z^V(Q^2; M_Z^2) = \frac{1}{N} \frac{4 \sin^2 \theta_W \cos^2 \theta_W}{4M_Z^2 \sin^2 \theta_W \cos^2 \theta_W} \frac{1}{(Q^2 - M_Z^2)^2 + M_Z^2 \Gamma_Z^2}; \quad (2.8)$$

$$\sigma_W^V(Q^2; M_W^2) = \frac{1}{N} \frac{4 \sin^2 \theta_W}{M_W^2 \sin^2 \theta_W} \frac{1}{(Q^2 - M_W^2)^2 + M_W^2 \Gamma_W^2}; \quad (2.9)$$

For completeness we also give the formula for the Z interference

$$\sigma_Z^V(Q^2; M_Z^2) = \frac{1}{N} \frac{4 \sin^2 \theta_W \cos^2 \theta_W}{6 \sin^2 \theta_W \cos^2 \theta_W} \frac{1}{Q^2} \frac{1}{(Q^2 - M_Z^2)^2 + M_Z^2 \Gamma_Z^2}; \quad (2.10)$$

In the above expression θ_W denotes the electroweak angle. Furthermore Γ_Z and Γ_W represent the total width of the Z and W boson respectively (sum over all decay channels) and $N = 3$ (SU(3), color). The partial widths due to the leptonic decay of the Z and W are given by

$$\Gamma_Z^{\ell\bar{\ell}} = \frac{M_Z (1 + (1 - 4 \sin^2 \theta_W)^2)}{48 \sin^2 \theta_W \cos^2 \theta_W}; \quad (2.11)$$

$$\Gamma_W^{\ell\bar{\ell}} = \frac{M_W}{12 \sin^2 \theta_W}; \quad (2.12)$$

In the case of W- and Z-production the total cross section can be obtained using the narrow width approximation while integrating (2.5) over Q^2 , i.e.

$$\frac{1}{(Q^2 - M_V^2)^2 + M_V^2 \Gamma_V^2} \approx \frac{1}{M_V \Gamma_V} \delta(Q^2 - M_V^2); \quad (2.13)$$

The total rates $\hat{\sigma}_{ij}^V$ (sum over all leptonic and hadronic decay channels) are now given by

$$\hat{\sigma}_{ij}^Z = \frac{1}{N} \frac{4 \sin^2 \theta_W \cos^2 \theta_W}{4 \sin^2 \theta_W \cos^2 \theta_W} \frac{1}{\hat{s}} \hat{W}_{ij}^Z(M_Z^2 = \hat{s}; M_Z^2; m_1^2; m_2^2); \quad (2.14)$$

$$\hat{\sigma}_{ij}^W = \frac{1}{N} \frac{4 \sin^2 \theta_W}{\sin^2 \theta_W} \frac{1}{\hat{s}} \hat{W}_{ij}^W(M_W^2 = \hat{s}; M_W^2; m_1^2; m_2^2); \quad (2.15)$$

When we consider the reaction where the vector boson decays into a specific lepton pair ℓ_1, ℓ_2 $\hat{\sigma}_{ij}^V$ in expressions (2.14), (2.15) has to be replaced by

$$\hat{\sigma}_{ij}^V \rightarrow \hat{\sigma}_{ij}^V B(V \rightarrow \ell_1 \ell_2); \quad (2.16)$$

where $B(V \rightarrow \psi_1 \psi_2)$ stands for the branching ratio

$$B(V \rightarrow \psi_1 \psi_2) = \frac{v \Gamma_{\psi_1 \psi_2}}{\Gamma_V}; \quad (2.17)$$

Notice that all particles into which the vector bosons decay are taken to be massless which is a good approximation since $M_Z \gg m_b$ and the top is too heavy to appear in the decay products.

Further since the electroweak radiative corrections to $\sin^2 \theta_W$ are non negligible it is better to replace $\sin^2 \theta_W$ appearing in the denominators of the above expressions by

$$\sin^2 \theta_W = \frac{P}{G_F \sqrt{2} M_W^2}; \quad (2.18)$$

where $G_F = 1.1667 \cdot 10^5 \text{ GeV}^{-2}$ (Fermi constant) whereas in the numerators we have put $\sin^2 \theta_W = 0.2258$.

The above definitions imply that the vector- and axial-vector couplings describing the strength of the coupling of the vector bosons to the quarks are hidden in the definition for \hat{W}_{ij}^V in (2.5). The same also holds for the elements of the Kobayashi-Maskawa matrix, denoted by $V_{q_1 q_2}$, which we approximate by retaining the Cabibbo angles only and putting the remaining angles and phases equal to zero.

In the case of the Born process as given by reaction (2.6) the DY-structure function becomes

$$\hat{W}_{q_1 q_2}^V = \left[\hat{Y}_{q_1 q_2} \right]^2 \left[v_q^V \right]^2 + \left[a_q^V \right]^2 \quad (1 \rightarrow); \quad (2.19)$$

with $V_{q_1 q_2} = 1$ in the case $V = \gamma, Z$. The vector- and axial-vector couplings are equal to

$$\begin{aligned} v_u &= \frac{2}{3}; & a_u &= 0; \\ v_d &= \frac{1}{3}; & a_d &= 0; \\ v_u^Z &= 1 - \frac{8}{3} \sin^2 \theta_W; & a_u^Z &= -1; \\ v_d^Z &= 1 + \frac{4}{3} \sin^2 \theta_W; & a_d^Z &= 1; \\ v_u^W &= v_d^W = \frac{1}{\sqrt{2}}; & a_u^W &= a_d^W = \frac{1}{\sqrt{2}}; \end{aligned} \quad (2.20)$$

We will now list all order α_s^2 parton cross sections due to heavy quark production contributing to reaction (2.1).

We start with the two-loop corrections to the Born process

$$q_1 + q_2 \rightarrow V; \quad (2.21)$$

which are presented by the graphs in Figs. 1 and 2. The first one (Fig. 1) contains a heavy quark in the triangular loop and it only contributes to Z-production. The

W does not contribute because of charge conservation and the same holds for the photon due to charge conjugation (Furry's theorem). The DY structure function is equal to [10]-[12]

$$W_{qq}^Z = (1 - \epsilon) a_q^Z a_Q^Z C_F T_f \frac{1}{2} \frac{s}{Q^2 - 4m^2} G_1(m^2=Q^2) + (4m^2 - Q^2) G_2(m^2=Q^2); \quad (2.22)$$

where C_F and T_f are the $SU(N)$ color factors: $C_F = \frac{N^2 - 1}{2N}$, $T_f = \frac{1}{2}$ and $q = u, d, s, c$, $Q = b, t$. The functions G_1 and G_2 are given in Eqs. (2.8) and (2.9) of [11] respectively. Notice that in expression (2.22) one has to sum over b and t in order to cancel the Adler-Bell-Jackiw axial anomaly.

The second two-loop correction to (2.21) is given by the vertex correction in Fig. 2. It contains the heavy quark loop contribution to the gluon self energy insertion in the vertex graph. The DY structure function becomes

$$W_{qq}^V = (1 - \epsilon) V_{q_1 q_2}^V \frac{1}{2} \frac{s}{Q^2 - 4m^2} F(Q^2; m^2); \quad (2.23)$$

where $F(Q^2; m^2)$ can be found in (A.1). The above expression contributes for all vector bosons and $V_{q_1 q_2}^V = 1$ when $V = \gamma, Z$.

Next we have the one-loop corrections to the two-to-two body processes (see Figs. 3 and 4)

$$q + q \rightarrow g + V; \quad (2.24)$$

$$g + q(q) \rightarrow q(q) + V; \quad (2.25)$$

They all contain the triangle heavy quark loop insertion which only contributes to Z -production for the same reasons as mentioned above (2.22). For process (2.24) (Fig. 3) the DY structure function reads

$$\hat{W}_{qq}^Z = a_q^Z a_Q^Z C_F T_f \frac{1}{2} \frac{s}{Q^2 - 4m^2} \left[\frac{1 + \epsilon}{1 - \epsilon} + 2 + 2\epsilon J_1(4m^2=s) - J_1(4m^2=Q^2) - \frac{4m^2}{s} J_2(4m^2=s) - J_2(4m^2=Q^2) \right]; \quad (2.26)$$

where J_1 and J_2 are given in Eqn. (2.12) of [11].

For process (2.25) (Fig. 4) we have the expression

$$\hat{W}_{qq}^Z = a_q^Z a_Q^Z T_f^2 \frac{1}{2} \frac{s}{Q^2 - 4m^2} \left[(Q^2 - 4m^2) H_1(s; Q^2; m^2) + (4m^2 - Q^2) H_2(s; Q^2; m^2) \right]; \quad (2.27)$$

with H_1 and H_2 defined in (2.18) and (2.19) of [11] respectively. Like for the DY structure function in (2.22) the above expressions (2.26) and (2.27) have to be summed

over b and t in order to cancel the axial anomaly.

The next contributions are given by the two to three body reactions (see Figs. 5 and 6)

$$q(k_1) + q(k_2) \rightarrow V(q) + Q_1(p_1) + Q_2(p_2); \quad (2.28)$$

$$g(k_1) + g(k_2) \rightarrow V(q) + Q_1(p_1) + Q_2(p_2); \quad (2.29)$$

Since at this moment experiments indicate that $m_t > m_b + M_W$ [9] W -production has to be treated in a way which differs from the usual procedure applied to Z - and γ -production. This is due to the instability of the top quark appearing in the internal lines of the Feynman graphs in Figs. 5 and 6 corresponding to the reactions

$$q + q \rightarrow t + t \quad (2.30)$$

$$b \rightarrow W^+ + b,$$

$$q + q \rightarrow t + t \quad (2.31)$$

$$b \rightarrow W + b,$$

$$g + g \rightarrow t + t \quad (2.32)$$

$$b \rightarrow W^+ + b,$$

$$g + g \rightarrow t + t \quad (2.33)$$

$$b \rightarrow W + b.$$

In this case the internal top quark line cannot be described by an ordinary Feynman propagator anymore. Therefore it has to be treated as a resonance which implies that the top quark propagator has to be replaced by a Breit-Wigner form. However this procedure leads to a violation of gauge invariance which is hard to remedy. In the case of the total cross section (2.15) one can resort to an approximation which will be presented at the end of this section.

Starting with Z - and γ -production which is described by the Feynman diagrams in Figs. 5 and 6 the DY structure function is given by

$$\hat{W}_{ij}^V = K_{ij} \frac{1}{8} \frac{s}{4} \frac{1}{\hat{s}} \int_0^Z d\hat{t}_1 \int_0^Z d\hat{u}_1 \int_0^1 d\sin^2 \theta \int_0^1 d\cos^2 \theta \int_0^1 d\sin^2 \theta \int_0^1 d\cos^2 \theta M_{ij}^V{}^2; \quad (2.34)$$

where $(i, j) = (q, q)$ or (g, g) . The symbol K_{ij} denotes the color factor which is given by $K_{qq} = C_F T_f$ and $K_{gg} = T_f^2$. In the definition of \hat{W}_{ij}^V an average over the initial spins and a sum over the final spins is understood. The Kallen function is defined by $\hat{s}(x; y; z) = x^2 + y^2 + z^2 - 2xy - 2xz - 2yz$ and the kinematical invariants \hat{s}_4 , \hat{t}_1 , and \hat{u}_1 are given by (see (2.28) and (2.29))

$$\hat{s}_4 = (p_1 + p_2)^2; \quad \hat{t}_1 = (k_2 - q)^2; \quad \hat{u}_1 = (k_1 - q)^2; \quad (2.35)$$

In addition to the above invariants the matrix element squared $M_{ij}^{V^2}$ depends on other kinematical variables which are analogous to the ones defined in Eqn. (4.2) of [13]. After having performed the traces the computation of $M_{ij}^{V^2}$ requires an intensive partial fractioning before the angular integration can be carried out. The angular integrals can be found in Appendix C of [13]. Notice that in the definition of \mathcal{M}^2 we have removed all the strong and electroweak coupling constants described by g_s , e , and g as defined in sections 10.6 and 14.5 of [14]. This also includes the typical factors which appear in the vertices like $ig_s T_a$, iev_q , $\frac{ig}{2}V_{q_1 q_2}$ ($v_q^W + s a_q^W$) and $\frac{ig}{4 \cos_w} (v_q^Z + s a_q^Z)$ (see Eqn. (2.20)). Here $V_{q_1 q_2}$ denotes the Kobayashi-Maskawa matrix element where only the Cabibbo angle θ_c has been put to be unequal to zero. All these factors are absorbed in the definition of the pointlike cross sections $\hat{\sigma}_V(Q^2; M_V^2)$ as presented in (2.7)–(2.9) except for the Cabibbo angles and the couplings v_q^V and a_q^V (2.20) which remain in \hat{W}_{ij}^V . In the case the vector boson couples to massless quarks they can be factored out too like in (2.19) but for massive quarks like the heavy flavors they remain in $M_{ij}^{V^2}$.

In the case $Q^2 \gg m^2$ ($m_1 = m_2 = m$) one can obtain analytic expressions for the DY structure functions \hat{W}_{qq}^V and \hat{W}_{gg}^V . For process (2.28) where the vector boson is radiated off the incoming light quark lines (see Figs. 5a,b) one obtains

$$\begin{aligned}
\hat{W}_{qq}^{V;(1)} \hat{\sigma}_V \frac{Q^2}{m^2} &= \mathcal{J}_{q_1 q_2}^2 \left(v_q^V{}^2 + a_q^V{}^2 \right) C_F T_f \frac{s}{4} \left(\frac{8}{3} \frac{1+\hat{\alpha}^2}{1-\hat{\alpha}^2} \ln^2 \frac{Q^2}{m^2} \right. \\
&+ \frac{1+\hat{\alpha}^2}{1-\hat{\alpha}^2} \frac{32}{3} \ln(1-\hat{\alpha}^2) - \frac{32}{3} \ln \hat{\alpha} - \frac{80}{9} - \frac{32}{3} (1-\hat{\alpha}^2) \ln \frac{Q^2}{m^2} \\
&+ \frac{1+\hat{\alpha}^2}{1-\hat{\alpha}^2} \frac{32}{3} \ln^2(1-\hat{\alpha}^2) - \frac{64}{3} \ln \hat{\alpha} \ln(1-\hat{\alpha}^2) + \frac{28}{3} \ln^2 \hat{\alpha} - \frac{160}{9} \ln(1-\hat{\alpha}^2) \\
&+ \frac{160}{9} \ln \hat{\alpha} - \frac{8}{3} \text{Li}_2(1-\hat{\alpha}^2) - \frac{32}{3} (2) + \frac{448}{27} - \frac{16}{3} (1-\hat{\alpha}^2) \\
&\left. - 4 \ln(1-\hat{\alpha}^2) - 4 \ln \hat{\alpha} - \frac{19}{3} - \frac{16}{3} \ln \hat{\alpha} + \frac{8}{3} (1+\hat{\alpha}^2) \text{Li}_2(1-\hat{\alpha}^2) + \frac{1}{2} \ln^2 \hat{\alpha} \right) :
\end{aligned} \tag{2.36}$$

If the parton cross section (2.5) is convoluted by the parton densities in order to compute the hadronic cross sections, as will be discussed in the next section, one approaches a singularity at $\hat{\alpha} = 1$. In this case one cannot neglect the mass m in the denominator anymore. The resulting terms which even can go as a power of the type $\ln^3 Q^2 = m^2$ will be partially cancelled by similar terms arising in the vertex correction (2.23) (see (A.3)). They all can be described by an expression proportional to a delta function which has to be added to expression (2.36). This expression reads as follows

$$\hat{W}_{qq}^{V;(2)} \hat{\sigma}_V \frac{Q^2}{m^2} = \mathcal{J}_{q_1 q_2}^2 \left(v_q^V{}^2 + a_q^V{}^2 \right) C_F T_f \frac{s}{4} (1-\hat{\alpha}^2) 4 \ln^2 \frac{Q^2}{m^2}$$

The polylogarithms of the type $\text{Li}_n(x)$, $S_{n,p}(x)$ are defined in [15].

$$\frac{68}{3} \ln \frac{Q^2}{m^2} + \frac{32}{3} (3) - 16 (2) + \frac{454}{9} : \quad (2.37)$$

Furthermore one has to replace in (2.36) the singular terms of the type $\ln^i(1 - \hat{x}) = (1 - \hat{x})$ by $\ln^i(1 - \hat{x}) = (1 - \hat{x})$ with the definition

$$\int_0^1 dx \frac{\ln^i(1 - x)}{1 - x} + f(x) = \int_0^1 dx \frac{\ln^i(1 - x)}{1 - x} (f(x) - f(1)) : \quad (2.38)$$

When the vector boson is radiated on the final state (see Figs. 5c,d) one finds in the limit $Q^2 \gg m^2$

$$\begin{aligned} \hat{W}_{qq}^{V;(3)} \left(\hat{x}, \frac{Q^2}{m^2} \right) &= \mathcal{J}_{q_1 q_2}^2 v_Q^V + a_Q^V C_F T_f \frac{s}{4} (1 + \hat{x})^2 \\ &\frac{32}{3} L_{\frac{1}{2}}(\hat{x}) - \frac{16}{3} (2) + \frac{8}{3} \ln^2 \hat{x} - \frac{32}{3} \ln \hat{x} \ln(1 + \hat{x}) \\ &+ \frac{8}{3} (3 + 4\hat{x} + 3\hat{x}^2) \ln \hat{x} + \frac{40}{3} (1 - \hat{x}^2) : \end{aligned} \quad (2.39)$$

Finally in the case of Z-production one can also find an asymptotic expression for the interference terms between diagrams 5a,b and 5c,d. It is given by [2, 11]

$$\hat{W}_{qq}^{Z;(4)} \left(\hat{x}, \frac{Q^2}{m^2} \right) = a_q^Z a_Q^Z C_F T_f \frac{s}{4} \left(16 \frac{1 + \hat{x}^2}{1 - \hat{x}} \ln \hat{x} + 32 \hat{x} \ln \hat{x} + 16(3 - \hat{x}) \right) : \quad (2.40)$$

For the gluon-gluon fusion process (2.29) (see Fig. 6) one finds the following asymptotic expression

$$\begin{aligned} \hat{W}_{gg}^{V;(1)} \left(\hat{x}, \frac{Q^2}{m^2} \right) &= \mathcal{J}_{q_1 q_2}^2 v_Q^V + a_Q^V T_f^2 \frac{s}{4} \left(f_8 (1 + 4\hat{x} + 4\hat{x}^2) \right. \\ &\ln \hat{x} + 16(1 - \hat{x})(1 + 3\hat{x}) g \ln \frac{Q^2}{m^2} + 32(1 + 4\hat{x} + 4\hat{x}^2) L_{\frac{1}{2}}(1 - \hat{x}) + \\ &\ln \hat{x} \ln(1 - \hat{x}) - \frac{1}{4} \ln^2 \hat{x} - 64(1 - \hat{x})(1 + 3\hat{x}) \ln(1 - \hat{x}) + \\ &8(1 + 8\hat{x} - 4\hat{x}^2) \ln \hat{x} + 4(1 - \hat{x})(7 + 67\hat{x}) \ln \frac{Q^2}{m^2} + 4(1 + 4\hat{x} + 4\hat{x}^2) \\ &16L_{\frac{1}{2}}(1 - \hat{x}) - 4L_{\frac{1}{2}}(1 - \hat{x}) \ln \hat{x} - 16L_{\frac{1}{2}}(1 - \hat{x}) \ln(1 - \hat{x}) + \\ &4 \ln^2 \hat{x} \ln(1 - \hat{x}) - 8 \ln^2(1 - \hat{x}) \ln \hat{x} + 4(1 + \hat{x}) - 8L_{\frac{1}{2}}(\hat{x}) + \end{aligned}$$

$$\begin{aligned}
& 8 \ln^2 \ln(1 + \frac{1}{N}) + 4(1 + \frac{1}{N})^2 \left[16S_{1;2}(\frac{1}{N}) - 16L_{\frac{1}{2}}(\frac{1}{N}) \ln(1 + \frac{1}{N}) \right. \\
& \quad \left. - 8(2) \ln(1 + \frac{1}{N}) + 12 \ln^2 \ln(1 + \frac{1}{N}) - 8 \ln^2(1 + \frac{1}{N}) \ln^2 \frac{1}{N} - 32(1 + 10\frac{1}{N} + \right. \\
& \quad \left. 7\frac{1}{N^2}) S_{1;2}(1 - \frac{1}{N}) - 32(1 + 2\frac{1}{N} + \frac{1}{N^2}) L_{\frac{3}{2}}(\frac{1}{N}) - 16(1 + 2\frac{1}{N} + \frac{1}{N^2}) \right] (3) \\
& \quad \left. + 16(5 + 4\frac{1}{N} + 14\frac{1}{N^2}) L_{\frac{1}{2}}(1 - \frac{1}{N}) + 32(2 + 4\frac{1}{N} + \frac{1}{N^2}) L_{\frac{1}{2}}(\frac{1}{N}) \ln^2 \frac{1}{N} + 16(2) \right. \\
& \quad \left. (3 + 10\frac{1}{N} + 10\frac{1}{N^2}) \ln^2 \frac{1}{N} + 16(5 + 9\frac{1}{N} + 12\frac{1}{N^2}) \right] (2) - \frac{8}{3} (3 + 8\frac{1}{N} + 8\frac{1}{N^2}) \ln^3 \frac{1}{N} \\
& \quad - 8(3 + 7\frac{1}{N} + 4\frac{1}{N^2}) \ln^2 \frac{1}{N} - 64(1 - \frac{1}{N})(1 + 3\frac{1}{N}) \ln(1 - \frac{1}{N}) + 16(1 + 8\frac{1}{N} + 4\frac{1}{N^2}) \\
& \quad \ln^2 \frac{1}{N} \ln(1 - \frac{1}{N}) - 4(23 + 64\frac{1}{N} + 105\frac{1}{N^2}) \ln^2 \frac{1}{N} + 8(1 - \frac{1}{N})(7 + 67\frac{1}{N}) \ln(1 - \frac{1}{N}) \\
& \quad - 8(1 - \frac{1}{N})(16 + 49\frac{1}{N}) \\
& \quad + \frac{N^2}{N^2 - 1} \left[4(1 + \frac{1}{N})^2 \left[16S_{1;2}(\frac{1}{N}) + 24L_{\frac{1}{2}}(\frac{1}{N}) + 16(3) \right. \right. \\
& \quad \left. \left. + \frac{16}{3} L_{\frac{1}{2}}(\frac{1}{N}) - 24L_{\frac{1}{2}}(\frac{1}{N}) \ln^2 \frac{1}{N} + 16L_{\frac{1}{2}}(\frac{1}{N}) \ln(1 + \frac{1}{N}) + 8(2) \ln(1 + \frac{1}{N}) \right. \right. \\
& \quad \left. \left. + \frac{8}{3} (2) - 12 \ln^2 \ln(1 + \frac{1}{N}) + 8 \ln^2(1 + \frac{1}{N}) \ln^2 \frac{1}{N} + \frac{16}{3} \ln^2 \ln(1 + \frac{1}{N}) \right. \right. \\
& \quad \left. \left. - 32(1 - \frac{1}{N})^2 S_{1;2}(1 - \frac{1}{N}) + \frac{8}{3} (2 + 2\frac{1}{N} + 25\frac{1}{N^2}) \ln^2 \frac{1}{N} - \frac{8}{3} (6 + 38\frac{1}{N} + 75\frac{1}{N^2}) \ln^2 \frac{1}{N} \right. \right. \\
& \quad \left. \left. - \frac{1}{3} (1 - \frac{1}{N})(188 + 764\frac{1}{N}) \right] : \tag{2.41}
\end{aligned}$$

As we will see in the next section some of the above approximation turn out to be very useful for Z-production accompanied with bb quarks because $Q^2 = M_Z^2 \gg m_b^2$. As has been discussed below (2.29) W-production has to be treated in a different way as has been done above for Z- and -production. Here one has to make a distinction between initial and final state emission of the W-boson. In the case the W-boson is radiated off from a light quark in the initial state, described by the graphs in Figs. 5a,b, the DY structure function is given by \hat{W}_{qq}^W in (2.34). However if the W-boson is the decay product of the top or anti-top quark in the final state like in Figs. 5c,d or Fig. 6 one has to resort to different methods. In this paper we are only interested in the total cross section. Hence we can follow the same procedure as is outlined in (2.13)-(2.15). First we neglect the graphs where the W is emitted from the bottom quark because the latter is far off-shell and apply the narrow width approximation to the Breit-Wigner form of the top quark in reactions (2.30) and

(2.31). This is a reasonable approach because the width of the top $\Gamma_t = 1.41 \text{ GeV}$ is much smaller than its mass $m_t = 174 \text{ GeV}$ [9]. Following the above procedure for W -production in quark-antiquark annihilation the total cross section is then given by

$$\sigma_{qq}^W = \sigma_{\text{tot}}(qq \rightarrow tt) B(t \rightarrow Wb); \quad (2.42)$$

with $B(t \rightarrow Wb) \approx 1$ and $\sigma_{\text{tot}}(qq \rightarrow tt)$ [19, 25] is equal to

$$\sigma_{\text{tot}}(qq \rightarrow tt) = \frac{4}{3} \frac{1}{s} \frac{1}{N} C_F T_f \frac{1}{s} \left[1 + \frac{4m^2}{s} \right] \left[1 + \frac{2m^2}{s} \right]; \quad (2.43)$$

In the case of the gluon-gluon fusion process (2.29) we proceed in the same way. Neglecting the emission of the W from the bottom quark and applying the narrow width approximation to reactions (2.32), (2.33) we get

$$\sigma_{gg}^W = \sigma_{\text{tot}}(gg \rightarrow tt) B(t \rightarrow Wb); \quad (2.44)$$

where $\sigma_{\text{tot}}(gg \rightarrow tt)$ is given by [19, 25]

$$\begin{aligned} \sigma_{\text{tot}}(gg \rightarrow tt) = & 4 \frac{1}{s} \frac{1}{N} T_f^2 \frac{1}{s} \left[1 + \frac{4m^2}{s} \right] \left[1 + \frac{4m^2}{s} \right] \\ & + \left[1 + \frac{4m^2}{s} \right] \frac{8m^4}{s^2} \ln y(s) + \frac{N^2}{N^2 - 1} \left[\frac{2}{3} + \frac{10m^2}{3s} \right] \left[1 + \frac{4m^2}{s} \right] \\ & + \frac{8m^4}{s^2} \ln y(s); \end{aligned} \quad (2.45)$$

with

$$y(s) = \frac{1 + \sqrt{1 - \frac{4m^2}{s}}}{1 - \sqrt{1 - \frac{4m^2}{s}}}; \quad (2.46)$$

^y Γ_t is related to m_t using the formula in [18].

3 Hadronic cross sections

In this section we want to discuss the heavy flavor (b and t) contribution to the total cross section of W - and Z -production at large hadron colliders. The energies and the colliders under study are given by $\sqrt{s} = 0.63 \text{ TeV}$ (SppS, pp), $\sqrt{s} = 1.8 \text{ TeV}$ (TEVATRON, pp) and $\sqrt{s} = 16 \text{ TeV}$ (LHC, pp). Investigated will be the part of the total cross section constituted by the heavy flavor contribution. We also want to know how the latter, which is of order $\frac{2}{s}$, compares with the light parton contribution calculated in the same order of perturbation theory which has been studied in the past (see [2, 3]). Finally we want to study the validity of the approximation for the total cross section of $H_1 + H_2 \rightarrow Z + b + b$ obtained from the formula in (2.36)–(2.41) which are calculated in the limit $M_Z^2 \gg m_b^2$.

The hadronic cross section is related to the partonic cross section (2.5) through the relation

$$\frac{d^v}{dQ^2} = \sum_{ij} \int_0^{z_1} dy_1 \int_0^{z_1} dy_2 \int_0^{z_1} dz \left(Y_{YZ} \right) Y_1 Y_2 f_i^{H_1}(y_1; \frac{2}{s}) f_j^{H_2}(y_2; \frac{2}{s}) \frac{d^v_{ij}}{dQ^2}(Q^2 = Y_1 Y_2 s; Q^2; m_1^2; m_2^2; \frac{2}{s}); \quad (3.1)$$

where $f_i^H(y; \frac{2}{s})$ denotes the density of parton i inside the hadron H which depends aside from y also on the factorization (renormalization) scale μ . Notice that for convenience we have put the renormalization scale equal to the factorization scale.

In the case heavy flavor production is treated in lowest order, as we do in this paper, $d^v = dQ^2$ is independent of the factorization scale (Born approximation). However since this approximation is of order $\frac{2}{s}$ it does depend on the renormalization scale. In the case of light partons in the initial and final state one has to perform mass factorization to $d^v_{ij} = dQ^2$ in order to remove the collinear divergences and this quantity has to be replaced by the DY coefficient function which has been calculated up to order $\frac{2}{s}$ in [2, 3]. Therefore in addition to the renormalization scale the latter also depends on the factorization scale.

In our calculations we have chosen the \overline{MS} -scheme for the coupling constant α_s as well as for the DY-coefficient function calculated up to order $\frac{2}{s}$ in [2]. For the parton densities we have chosen the \overline{MS} -version of the set MR S(H) [26] with $\frac{(4)}{MS} = 230 \text{ MeV}$. Furthermore we use the two-loop corrected running coupling constant α_s with the QCD scale mentioned above. Since we only consider top and bottom quark production we have put the number of light flavors equal to four, i.e. $n_f = 4$. Finally we have set the factorization (renormalization) scale $\mu^2 = Q^2$ where $Q^2 = M_V^2$. For the electroweak parameters we have taken the following values: $M_Z = 91.196 \text{ GeV}$, $M_W = 80.24 \text{ GeV}$, $G_F = 1.1667 \cdot 10^5 \text{ GeV}^{-2}$, $\sin^2 \theta_W = 0.2258$ and $\sin^2 \theta_C = 0.0484$. The masses of the heavy flavors are given by $m_b = 5 \text{ GeV}$ and $m_t = 174 \text{ GeV}$.

To calculate the total cross section for Z-production we have integrated expression (3.1) over Q^2 and used the narrow width approximation (2.14). In tables 1–3 we have listed the various contributions coming from the partonic subprocesses discussed in the previous section and compared them with the light parton cross section corrected

up to order $\frac{2}{s}$. The tables reveal that at smaller energies, i.e. $\sqrt{s} = 0.63 \text{ TeV}$ the total heavy flavor cross section is dominated by the vertex correction (2.22) given by Fig. 1 and the subprocess $q + \bar{q} \rightarrow Z + b + \bar{b}$ (2.34) depicted in Fig. 5. As we will show later on the importance of the last process is wholly due to initial state radiation (Figs. 5a,b). At larger energies like $\sqrt{s} = 1.8 \text{ TeV}$ also the process $g + g \rightarrow Z + b + \bar{b}$ (2.34) (Fig. 6) becomes important. The latter even overwhelms the other reactions when $\sqrt{s} = 16 \text{ TeV}$ (LHC). This can be traced back to the gluon density which steeply rises at very small $k = M_V^2 = s$. Finally we observe that the processes with top quarks in the final state are completely unimportant which is due to the limited phase space available even for energies as large as $\sqrt{s} = 16 \text{ TeV}$ (LHC).

The reason that the virtual correction in Fig. 1 plays an important role can be inferred from the expression in (2.22). Here the first term G_1 only contributes in the case of the bottom loop ($M_Z^2 > 4m_b^2$) whereas the second term G_2 only contributes for the top loop ($M_Z^2 < 4m_t^2$). In [11] it has been shown that for $Q^2 \gg m^2$ the function G_1 vanishes like

$$G_1 \sim \frac{m^2}{Q^2} \rightarrow 0 \quad \frac{m^2}{Q^2}; \quad (3.2)$$

whereas the function G_2 has the following asymptotic behavior for $m^2 \gg Q^2$

$$G_2 \sim \frac{m^2}{Q^2} \left[3 \ln \frac{Q^2}{m^2} - 2 \right] + \frac{21}{2} + O\left(\frac{Q^2}{m^2}\right); \quad (3.3)$$

which means that this correction is dominated by the top-loop contribution.

In tables 1-3 we have also listed the results coming from the light parton contribution calculated in [2]. We observe that the heavy flavor part of the DY cross section is very small and it amounts to 0.2% ($\sqrt{s} = 0.63 \text{ TeV}$), 0.3% ($\sqrt{s} = 1.8 \text{ TeV}$), 1% ($\sqrt{s} = 16 \text{ TeV}$) of the light quark contribution. Even if we compare the heavy flavor part, which is an order $\frac{2}{s}$ correction, with the corresponding light parton contribution in the same order of perturbation theory one discovers that it is very small except when the energy gets very large. It amounts to 5% ($\sqrt{s} = 0.63 \text{ TeV}$), 11% ($\sqrt{s} = 1.8 \text{ TeV}$), and 770% (absolute value) ($\sqrt{s} = 16 \text{ TeV}$) of the $\frac{2}{s}$ correction to the cross section which is due to light partons. This means that only at LHC energies heavy flavor production is more important than the light parton subprocesses contributing in order $\frac{2}{s}$.

For the W -cross section we proceed in the same way as for Z -production except that here we also have to make the narrow width approximation for the top quark. This is needed when the W is radiated off the top-quark in the final state exhibited by the graphs in Figs. 5c,d and 6. Furthermore the graphs containing the triangle heavy flavor loop like Figs. 1, 3, and 4 do not contribute. The results are given in tables 4-6. Like in the case of Z -production the process $q_1 + \bar{q}_2 \rightarrow W + b + \bar{b}$ (2.34) (Figs. 5a,b) is dominant at lower energies although also the vertex correction (2.23) contributes a little bit. When the energy gets larger like in the case of LHC also the process $g + g \rightarrow t + \bar{t}$ with $t \rightarrow W + b$ and $\bar{t} \rightarrow W + \bar{b}$ (2.44) (Fig. 6) becomes important due to the gluon density which becomes very large at small $k = M_W^2 = s$. As in Z -production the heavy flavors give a small contribution to the W -cross section. The latter is of the

same magnitude as in the Z-cross section and it amounts to 0.1% ($\sqrt{s} = 0.63 \text{ TeV}$), 0.1% ($\sqrt{s} = 1.8 \text{ TeV}$), and 0.2% ($\sqrt{s} = 16 \text{ TeV}$) of the light parton contribution. If we make a comparison with the order $\frac{2}{3}$ part of the light parton contribution these numbers become 2%, 6%, and 90% respectively which are however smaller than in the case of Z-production.

Besides vector boson production we have also studied the heavy flavor part of the DY cross section $d = dQ^2$ at small Q^2 ($Q^2 < 60 \text{ GeV}$) where the virtual photon dominates the cross section. In Fig. 7 we have plotted the ratio R

$$R(Q^2) = \frac{\frac{d}{dQ^2}(u;d;s;c;g) + \frac{d}{dQ^2}(t;b)}{\frac{d}{dQ^2}(u;d;s;c;g)}; \quad (3.4)$$

at three different energies, i.e. $\sqrt{s} = 0.63; 1.8; 16 \text{ TeV}$. Like in the case of Z- and W-boson production the contribution of the heavy flavors to the DY cross section is very small. When the energy increases it grows from 0.1% to 0.5% of the part constituted by the light parton contributions.

Using the MRS(H) [26] parton densities we also calculate the cross sections for Z- and W-production where the lepton pair into which the vector boson decays is measured. The results are presented in table 7 (SppS, $\sqrt{s} = 0.63 \text{ TeV}$) and table 8 (TEVA-TRON, $\sqrt{s} = 1.8 \text{ TeV}$). They are obtained by multiplying the total cross sections σ^Z and σ^W in tables 1 to 6 by the branching ratios $B(Z \rightarrow e^+e^-) = 3.35 \cdot 10^2$ and $B(W \rightarrow e_e) = 0.109$ respectively. Furthermore we have also listed the experimental data obtained from the groups UA1 [27], UA2 [28] (SppS) and CDF [29] (TEVA-TRON). As is expected from the previous discussion the contribution from the heavy flavors b and t to the cross section is extremely small when compared with the light parton part.

Before concluding this section we have also studied the cross sections obtained from (2.36)-(2.41) which are derived in the limit $Q^2 \gg m^2$. In practice these formulae are only applicable to the reaction $H_1 + H_2 \rightarrow Z + b + \bar{b}$ where $M_Z^2 \gg m_b^2$. This inequality does not apply to top production also when the Z is replaced by the W. In the case a photon appears in the intermediate state the above formulae are also not very useful because in the region $Q^2 \gg m^2$ the production rate is too low. In table 9 we have compared the results obtained from the exact cross section represented by (2.23), (2.34) with those predicted by the asymptotic formula in (2.36)-(2.41). First the table shows that the whole contribution to the cross section of the subprocess $q + \bar{q} \rightarrow Z + b + \bar{b}$ is given by the initial state radiation of the Z-boson as depicted in Figs. 5a,b which also includes the virtual contribution in Fig. 2. This is due to the large logarithmic terms $\ln^k(Q^2 = m^2)$ which show up in (2.36) and (2.37). Furthermore the approximations to the initial state radiation process work rather well in particular when the energy increases. The difference between the exact (2.23), (2.34) and the approximate cross sections (2.36), (2.37) amounts to 30% ($\sqrt{s} = 0.63 \text{ TeV}$), 17% ($\sqrt{s} = 1.8 \text{ TeV}$) and 16% ($\sqrt{s} = 16 \text{ TeV}$) of the exact value. The main reason for the difference is that the cubic logarithmic term $\ln^3(Q^2 = m^2)$, arising in the exact expressions (2.23), (2.34) in the limit $Q^2 \gg m^2$, will only cancel when m^2 is taken

to be really small with respect to Q^2 . This is apparently not the case for $Q^2 = M_Z^2$ and $m^2 = m_b^2$. Therefore the sum of the two exact expressions is not quite equal to the sum of the approximations (2.36) and (2.37) which behaves asymptotically like $\ln^2(Q^2=m^2)$. In practice the asymptotic limit is only reached for $m^2 < 1(\text{GeV}=c)^2$ which is an order of magnitude less than $m^2 = (5\text{GeV}=c)^2$. A similar problem shows up in the contribution originating from the interference between initial state (Figs. 5a,b) and final state (Figs. 5c,d) radiation of the vector boson. In spite of the fact that here no large logarithms of the type $\ln^k(Q^2=m^2)$ appear in the final expression (2.40) the various integrals contributing to the interference term contain these type of logarithms so that in this case one observes an incomplete cancellation too. From table 9 we infer that the approximation to the interference term is not so bad when $\sqrt{s} = 0.63\text{TeV}$ but it becomes worse at higher energies. Apart from the incomplete cancellation mentioned above this is also due to the fact that the quality of the approximation depends on the values for $\hat{s} = y_1 y_2 s$ in the partonic cross section $d\hat{\sigma} = dQ^2$ (3.1). When the energy \sqrt{s} increases it may happen that the product of the parton densities in (3.1) probe the \hat{s} -region where the approximation fails. Fortunately the interference term gives a negligible contribution to the cross section of $q + q \rightarrow Z + b + b$. The latter also holds for the final state radiation of the Z-boson as depicted by the graphs in Figs. 5c,d. However here the approximation to the cross section (2.34) as given by (2.39) becomes excellent which is independent of the energies under consideration. The most simple explanation for this phenomenon is that here large logarithms of the type $\ln^k(Q^2=m^2)$ neither appear in the final result (2.39) nor in the separate integrals contributing to this expression. Therefore in this case no cancellation of large logarithmic terms has to occur. Finally table 9 reveals that the approximation to the cross section of the gluon-gluon fusion process $g + g \rightarrow Z + b + b$ (Fig. 6) turns out to be very good for all energies under consideration. Although the approximate cross section (2.41) behaves quadratically in $\ln(Q^2=m^2)$ it is closer to the exact result as discovered for the initial state radiation of the Z-boson in $q + q \rightarrow Z + b + b$. This is mainly due to the fact that in the former process no cancellation of leading logarithmic terms occur.

In general we can conclude that irrespective of the energies considered the approximations work rather well for Z-production accompanied by bottom quarks although this statement is more valid for $g + g \rightarrow Z + b + b$ (Fig. 6) than for $q + q \rightarrow Z + b + b$ (Fig. 5). Since the large logarithms $\ln^k(Q^2=m^2)$ dominate the cross sections for $\sqrt{s} > 1.8\text{TeV}$ the bottom can be treated as a light quark. Further we have also studied the limit $Q^2 \gg m^2$ for the charmed quark cross sections. In this case the approximations (2.36)–(2.41) are even better than for bottom production. This even holds for $\sqrt{s} = 0.63\text{TeV}$. The logarithms of the type $\ln(Q^2=m^2)$ dominate the charm and bottom cross sections and they give rise to large corrections. Therefore they have to be removed by mass factorization and subsequently to be absorbed, after resummation via the renormalization group equations, into the charm and bottom densities in the hadron.

Summarizing the content of this paper we have computed all order $\frac{2}{s}$ contributions to the DY cross section which can be attributed to heavy flavors. All virtual as well as radiative processes have been considered. In this way we have extended the work

done in [10, 11] where only the contributions characteristic for Z-production have been considered.

From the results obtained in this work one can conclude that the contributions of the heavy flavors b and t to the DY cross section in particular to vector boson production are very small. They are on the one percent level in the case of Z-production provided the energy is very large which will only happen when the LHC is put into operation. Furthermore we have shown that for $\sqrt{s} > 1.8 \text{ TeV}$ the cross sections (2.36)–(2.41) derived in the limit $Q^2 \gg m^2$ can be applied to Z-production. This means that the bottom quark can be treated as a light flavor at large collider energies. The heavy flavor cross sections will only become observable if the vector boson as well as the heavy quarks are detected. This will happen for the LHC where the process $p + p \rightarrow Z + b + \bar{b}$ constitutes an important background for Higgs production [30].

Appendix A

In this appendix we present the two-loop vertex correction defined by $F(Q^2; m^2)$ in (2.23). It contains the gluon selfenergy contribution with the heavy flavors appearing in the subloop (Fig. 2). The vertex correction reads

$$\begin{aligned}
 F(Q^2; m^2) = & \frac{440m^2}{9Q^2} + \frac{530}{27} \ln \frac{Q^2}{m^2} + x \left[\frac{184m^2}{9Q^2} + \frac{76}{9} \right. \\
 & 2\text{Li}_2 \left(\frac{x-1}{x+1} \right) - 2(2) + \frac{1}{2} \ln^2 \frac{x-1}{x+1} \left. + 16 \frac{m^4}{Q^4} \right] \frac{8}{3} \\
 & 2\text{Li}_3 \left(\frac{x-1}{x+1} \right) + 2(3) \left[\frac{1}{6} \ln^3 \frac{x-1}{x+1} + 2(2) \ln \frac{x-1}{x+1} \right] + \frac{952m^2}{9Q^2} \\
 & + \frac{3355}{81}; \tag{A 1}
 \end{aligned}$$

where

$$x = \frac{s}{1 + 4 \frac{m^2}{Q^2}}; \tag{A 2}$$

Further the following asymptotic expansions turn out to be useful. In the limit $m^2 \ll Q^2$ one obtains the expansion

$$\begin{aligned}
 F(Q^2; m^2) \underset{m \ll Q}{=} & \frac{4}{9} \ln^3 \frac{Q^2}{m^2} + \frac{38}{9} \ln^2 \frac{Q^2}{m^2} + \frac{16}{3} (2) \frac{530}{27} \ln \frac{Q^2}{m^2} \\
 & + \frac{3355}{81} - \frac{152}{9} (2) - \frac{16}{3} (3); \tag{A 3}
 \end{aligned}$$

In the case that $m^2 \gg Q^2$ the vertex correction behaves like

$$F(Q^2; m^2) \underset{m \gg Q}{=} \frac{Q^2}{m^2} \left[\frac{176}{225} - \frac{8}{45} \ln \frac{Q^2}{m^2} \right]; \tag{A 4}$$

which shows that heavy flavors decouple from $F(Q^2; m^2)$ when the quark mass gets infinite.

References

- [1] S.D. Drell and T.M. Yan, *Phys. Rev. Lett.* 25 (1970) 316
- [2] R. Hamberg, W.L. van Neerven and T. Matsuura, *Nucl. Phys. B* 359 (1991) 343
- [3] W.L. van Neerven and E.B. Zijlstra, *Nucl. Phys. B* 382 (1992) 11
- [4] T. Matsuura and W.L. van Neerven, *Z. Phys. C* 38 (1988) 623
- [5] T. Matsuura, S.C. van der Marck and W.L. van Neerven, *Nucl. Phys. B* 319 (1989) 570
- [6] P.J. Rijken and W.L. van Neerven, *Phys. Rev. D* 51 (1995) 44
- [7] P.B. Arnold and M.H. Reno, *Nucl. Phys. B* 319 (1989) 37, Erratum *Nucl. Phys. B* 330 (1990) 284
- [8] R.J. Gonçalves, J. Pawłowski and C.F. Wai, *Phys. Rev. D* 40 (1989) 2245
- [9] F. Abe et al. (CDF Collaboration), *Phys. Rev. D* 50 (1994) 2966
- [10] D.A. Dicus and S.S.D. Willenbrock, *Phys. Rev. D* 34 (1986) 148
- [11] R.J. Gonçalves, E.M. Hung and J. Pawłowski, *Phys. Rev. D* 46 (1992) 4930
- [12] B.A. Kniehl and J.H. Kühn, *Nucl. Phys. B* 329 (1990) 547
- [13] W. Beenakker, H. Kuijf, W.L. van Neerven and J. Smith, *Phys. Rev. D* 40 (1989) 54
- [14] D. Bailin and A. Love, "Introduction to Gauge Field Theory", Revised edition 1993, J.W. Arrowsmith, Ltd. Bristol
- [15] L. Lewin, "Polylogarithms and Associated Functions" (North Holland, Amsterdam 1983)
- [16] R. Barbieri, J.A. Mignaco and E. Remiddi, *Nuovo Cim.* 11A (1972) 824
- [17] A. Devoto and D.W. Duke, *Riv. Nuovo Cim.* 7-6 (1984) 1
- [18] A. Denner and T. Sack, *Nucl. Phys. B* 358 (1991) 46
- [19] L.M. Jones and H. Wylid, *Phys. Rev. D* 17 (1978) 782
- [20] M. Glück, J.F. Owens and E. Reya, *Phys. Rev. D* 17 (1978) 2324
- [21] J. Babcock, D. Sivers and S. Wolfram, *Phys. Rev. D* 18 (1978) 162
- [22] H. Georgi et al., *Ann. Phys. (NY)* 114 (1978) 273
- [23] B.L. Combridge, *Nucl. Phys. B* 151 (1979) 429

- [24] K .Hagiwara and T .Yoshino, Phys. Lett. 80B (1979) 282
- [25] E .Laenen, J. Sm ith and W .L. van Neerven, NuclPhys B 369 (1992) 543
- [26] A D .M artin, W .J. Stirling and R G .Roberts, Phys. Rev. D 50 (1994) 6734
- [27] C .A lba jar et al. (UA 1 Collaboration), Phys. Lett. B 253 (1991) 503
- [28] J. A ltti et al. (UA 2 Collaboration), Phys. Lett. B 256 (1991) 365
- [29] F .A be et al. (CDF Collaboration), Phys. Rev. Lett. 69 (1992) 28
- [30] J F .G union, H E .H aber, G .K ane and S. D aw son, "The H iggs H unter's G uide",
Frontiers in Physics, Addison-W esley Pub. Co. 1990.

Table 1

Contributions to the total cross section for Z-production at $\sqrt{s} = 0.63 \text{ TeV}$ ($M_Z = 91.1876 \text{ GeV}$).

subprocess	equation	σ^Z (nb)
$q+q \rightarrow Z$	(2.22)	$3.13 \cdot 10^3$
$q+q \rightarrow Z$	(2.23)	$1.40 \cdot 10^4$
$q+q \rightarrow Z+g$	(2.26)	$1.13 \cdot 10^4$
$g+q(q) \rightarrow Z+q(q)$	(2.27)	$1.77 \cdot 10^5$
$q+q \rightarrow Z+b+b$	(2.34)	$1.47 \cdot 10^3$
$q+q \rightarrow Z+t+t$	(2.34)	$1.35 \cdot 10^{11}$
$g+g \rightarrow Z+b+b$	(2.34)	$6.39 \cdot 10^5$
$g+g \rightarrow Z+t+t$	(2.34)	$1.25 \cdot 10^{16}$
$\sigma^Z(b;t)$		$4.90 \cdot 10^3$
$\sigma^Z(u;d;s;c;g) = 1.54 \text{ (Born)} + 0.41 \text{ (O (s))} + 0.10 \text{ (O (s))} = 2.05$		

Table 2

Contributions to the total cross section for Z-production at $\sqrt{s} = 1.8 \text{ TeV}$ ($M_Z = 91.1876 \text{ GeV}$).

subprocess	equation	σ^Z (nb)
$q+q \rightarrow Z$	(2.22)	$5.33 \cdot 10^3$
$q+q \rightarrow Z$	(2.23)	$4.86 \cdot 10^4$
$q+q \rightarrow Z+g$	(2.26)	$3.67 \cdot 10^4$
$g+q(q) \rightarrow Z+q(q)$	(2.27)	$1.61 \cdot 10^4$
$q+q \rightarrow Z+b+b$	(2.34)	$8.57 \cdot 10^3$
$q+q \rightarrow Z+t+t$	(2.34)	$3.58 \cdot 10^6$
$g+g \rightarrow Z+b+b$	(2.34)	$4.71 \cdot 10^3$
$g+g \rightarrow Z+t+t$	(2.34)	$5.50 \cdot 10^8$
$\sigma^Z(b;t)$		$1.93 \cdot 10^2$
$\sigma^Z(u;d;s;c;g) = 5.34 \text{ (Born)} + 1.05 \text{ (O (s))} + 0.17 \text{ (O (s))} = 6.56$		

Table 3

Contributions to the total cross section for Z -production at $\sqrt{s} = 16 \text{ TeV}$ ($\sqrt{s} M_Z = 0.107$).

subprocess	equation	σ^Z (nb)
$q + q \rightarrow Z$	(2.22)	$1.21 \cdot 10^2$
$q + q \rightarrow Z$	(2.23)	$5.02 \cdot 10^3$
$q + q \rightarrow Z + g$	(2.26)	$8.06 \cdot 10^4$
$g + q(q) \rightarrow Z + q(q)$	(2.27)	$1.57 \cdot 10^3$
$q + q \rightarrow Z + b + b$	(2.34)	$9.28 \cdot 10^2$
$q + q \rightarrow Z + t + t$	(2.34)	$3.17 \cdot 10^4$
$g + g \rightarrow Z + b + b$	(2.34)	$5.85 \cdot 10^1$
$g + g \rightarrow Z + t + t$	(2.34)	$9.23 \cdot 10^4$
$\sigma^Z(b; t)$		$6.95 \cdot 10^1$
$\sigma^Z(u; d; s; c; g) = 55.2 \text{ (Born)} + 7.45 \text{ (} \alpha_s \text{)} + 0.09 \text{ (} \alpha_s^2 \text{)} = 62.6$		

Table 4

Contributions to the total cross section for $W^+ + W^-$ -production at $\sqrt{s} = 0.63 \text{ TeV}$ ($\sqrt{s} M_W = 0.109$).

subprocess	equation	σ^W (nb)
$q_1 + q_2 \rightarrow W$	(2.23)	$1.32 \cdot 10^3$
$q_1 + q_2 \rightarrow W + b + b$	(2.34)	$4.11 \cdot 10^3$
$q_1 + q_2 \rightarrow W + t + t$	(2.34)	$1.94 \cdot 10^{11}$
$q + q \rightarrow t(t) + t(t)$ $b \rightarrow W^+ (W^-) + b(b)$	(2.42)	$1.43 \cdot 10^6$
$g + g \rightarrow t(t) + t(t)$ $b \rightarrow W^+ (W^-) + b(b)$	(2.44)	$1.52 \cdot 10^8$
$\sigma^W(b; t)$		$5.43 \cdot 10^3$
$\sigma^W(u; d; s; c; g) = 5.09 \text{ (Born)} + 1.34 \text{ (} \alpha_s \text{)} + 0.33 \text{ (} \alpha_s^2 \text{)} = 6.76$		

Table 5

Contributions to the total cross section for $W^+ + W^-$ production at $\sqrt{s} = 1.8 \text{ TeV}$
 $(\sqrt{s} M_W) = 0.109$.

subprocess	equation	σ^W (nb)
$q_1 + q_2 \rightarrow W$	(2.23)	$4.67 \cdot 10^3$
$q_1 + q_2 \rightarrow W + b + b$	(2.34)	$2.51 \cdot 10^2$
$q_1 + q_2 \rightarrow W + t + t$	(2.34)	$6.36 \cdot 10^6$
$q + q \rightarrow t(t) + t(t)$ $b \rightarrow W^+ (W^-) + b(b)$	(2.42)	$1.10 \cdot 10^3$
$g + g \rightarrow t(t) + t(t)$ $b \rightarrow W^+ (W^-) + b(b)$	(2.44)	$1.28 \cdot 10^4$
$\sigma^W(b; t)$		$3.10 \cdot 10^2$
$\sigma^W(u; d; s; c; g) = 18.0 \text{ (Born)} + 3.47 \text{ (O}(\sqrt{s})) + 0.50 \text{ (O}(\frac{2}{s})) = 22.0$		

Table 6

Contributions to the total cross section for $W^+ + W^-$ production at $\sqrt{s} = 16 \text{ TeV}$
 $(\sqrt{s} M_W) = 0.109$.

subprocess	equation	σ^W (nb)
$q_1 + q_2 \rightarrow W$	(2.23)	$4.79 \cdot 10^2$
$q_1 + q_2 \rightarrow W + b + b$	(2.34)	$2.76 \cdot 10^1$
$q_1 + q_2 \rightarrow W + t + t$	(2.34)	$6.26 \cdot 10^4$
$q + q \rightarrow t(t) + t(t)$ $b \rightarrow W^+ (W^-) + b(b)$	(2.42)	$2.00 \cdot 10^2$
$g + g \rightarrow t(t) + t(t)$ $b \rightarrow W^+ (W^-) + b(b)$	(2.44)	$1.77 \cdot 10^1$
$\sigma^W(b; t)$		$5.22 \cdot 10^1$
$\sigma^W(u; d; s; c; g) = 185 \text{ (Born)} + 24.8 \text{ (O}(\sqrt{s})) + 0.6 \text{ (O}(\frac{2}{s})) = 209$		

Table 7

B_Z^Z and B_W^W for the SppS [27, 28] with $B_Z = B(Z \rightarrow e^+e^-) = 3.35 \cdot 10^2$ and $B_W = B(W \rightarrow e_e) = 0.109$, $\sqrt{s} = 0.63 \text{ TeV}$.

	B_Z^Z (pb)	B_W^W (pb)
UA 1	58.6 7.8 8.4	609 41 94
UA 2	65.6 4.0 3.8	682 12 40
B_V^V (u;d;s;c;g)	68.7	737
B_V^V (b;t)	0.164	0.592

Table 8

B_Z^Z and B_W^W for the TEVATRON [29] with $B_Z = B(Z \rightarrow e^+e^-) = 3.35 \cdot 10^2$ and $B_W = B(W \rightarrow e_e) = 0.109$, $\sqrt{s} = 1.8 \text{ TeV}$.

	B_Z^Z (nb)	B_W^W (nb)
CDF	0.214 0.011 0.020	2.20 0.04 0.20
B_V^V (u;d;s;c;g)	0.220	2.40
B_V^V (b;t)	$6.47 \cdot 10^4$	$3.38 \cdot 10^3$

Table 9

Comparison of the exact versus approximate cross sections for Z- and bb-production ($\mu_s(M_Z) = 0.107$).

$\sqrt{s} = 0.63 \text{ TeV}$						
	$\sigma_{\text{exact}} \text{ (nb)}$			$\sigma_{\text{app}} \text{ (nb)}$		
q+q! Z+b+b	1.58	10^3	(2.23), (2.34)	1.11	10^3	(2.36), (2.37)
	2.41	10^6	(2.34)	2.48	10^6	(2.39)
	9.09	10^6	(2.34)	1.26	10^5	(2.40)
g+g! Z+b+b	6.39	10^5	(2.34)	5.80	10^5	(2.41)
$\sqrt{s} = 1.8 \text{ TeV}$						
	$\sigma_{\text{exact}} \text{ (nb)}$			$\sigma_{\text{app}} \text{ (nb)}$		
q+q! Z+b+b	8.88	10^3	(2.23), (2.34)	7.40	10^3	(2.36), (2.37)
	4.31	10^5	(2.34)	4.35	10^5	(2.39)
	1.40	10^5	(2.34)	2.14	10^5	(2.40)
g+g! Z+b+b	4.71	10^3	(2.34)	4.56	10^3	(2.41)
$\sqrt{s} = 16 \text{ TeV}$						
	$\sigma_{\text{exact}} \text{ (nb)}$			$\sigma_{\text{app}} \text{ (nb)}$		
q+q! Z+b+b	9.54	10^2	(2.23), (2.34)	8.01	10^2	(2.36), (2.37)
	5.93	10^4	(2.34)	5.97	10^4	(2.39)
	6.88	10^6	(2.34)	2.30	10^5	(2.40)
g+g! Z+b+b	5.85	10^1	(2.34)	5.77	10^1	(2.41)

Figure captions

Fig. 1 Two-loop graph, containing the heavy flavors in the triangular subloop, which contributes to the subprocess $q + q \rightarrow Z + \gamma$ (2.22).

Fig. 2 Two-loop graphs, containing the heavy flavors in the gluon self energy, which contributes to the subprocess $q + q \rightarrow V$ (2.23).

Fig. 3 One-loop graph with the heavy flavors in the triangle contributing to the subprocess $q + q \rightarrow Z + g$ (2.26).

Fig. 4 One-loop graph with the heavy flavors in the triangle contributing to the subprocess $g + q(q) \rightarrow Z + q(q)$ (2.27).

Fig. 5 Diagrams contributing to the subprocess $q + q \rightarrow V + Q_1 + Q_2$; a, b: initial state radiation; c, d: final state radiation (2.34).

Fig. 6 Diagrams contributing to the subprocess $g + g \rightarrow V + Q_1 + Q_2$ (2.34).

Fig. 7 The heavy flavor content, represented by R (3.4), of the cross section $d\sigma = dQ^2$ for the processes: $p + p \rightarrow \gamma + X$ at $\sqrt{s} = 0.63 \text{ TeV}$ (solid line), $\sqrt{s} = 1.8 \text{ TeV}$ (dotted line) and $p + p \rightarrow \gamma + X$ at $\sqrt{s} = 16 \text{ TeV}$ (dashed line).

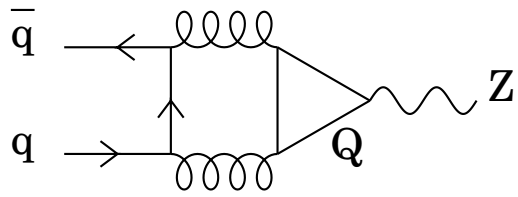


Fig. 1

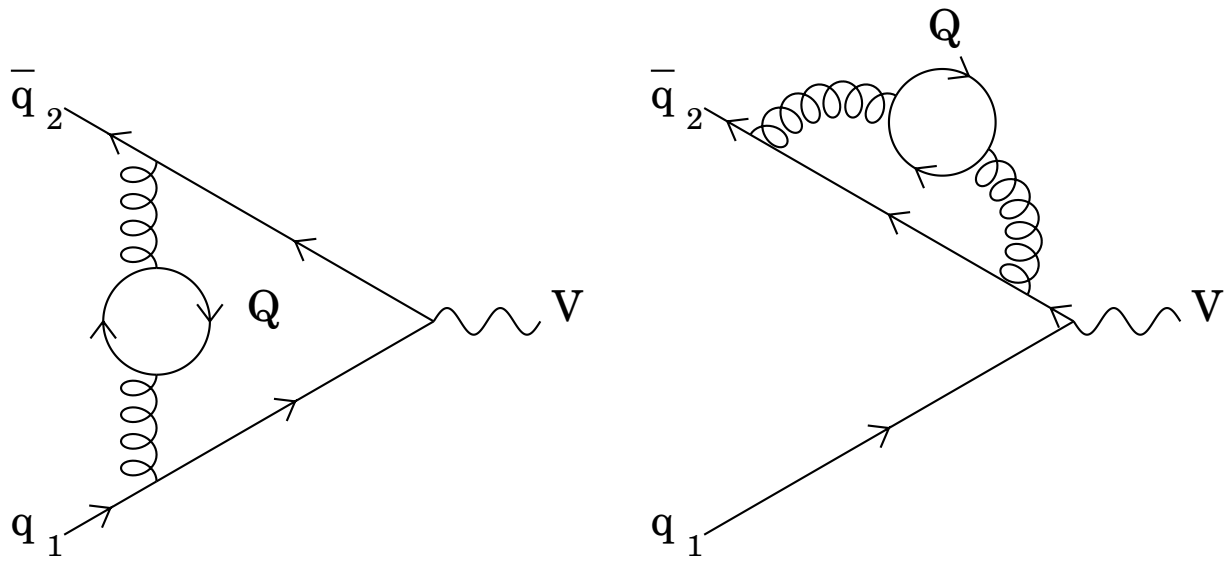


Fig. 2

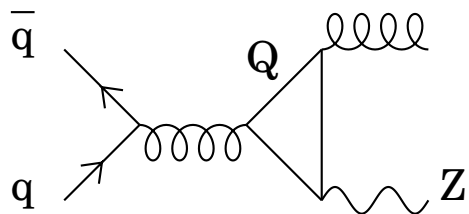


Fig. 3

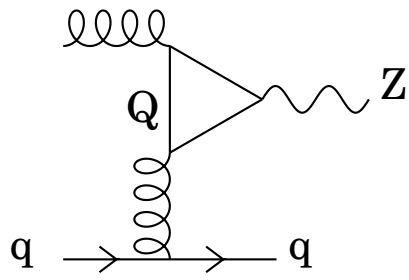


Fig. 4

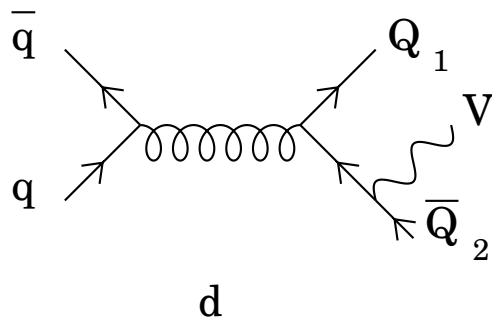
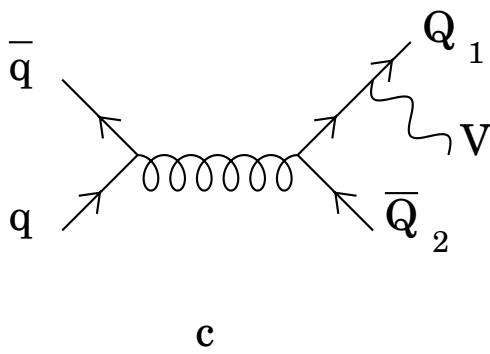
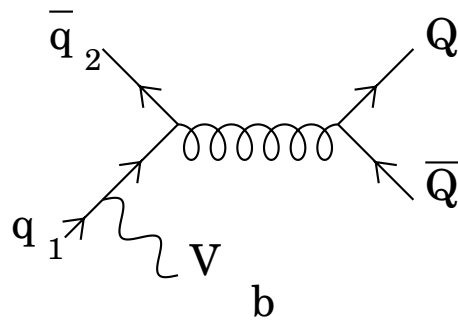
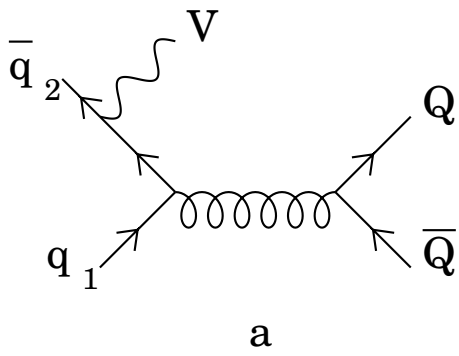


Fig. 5

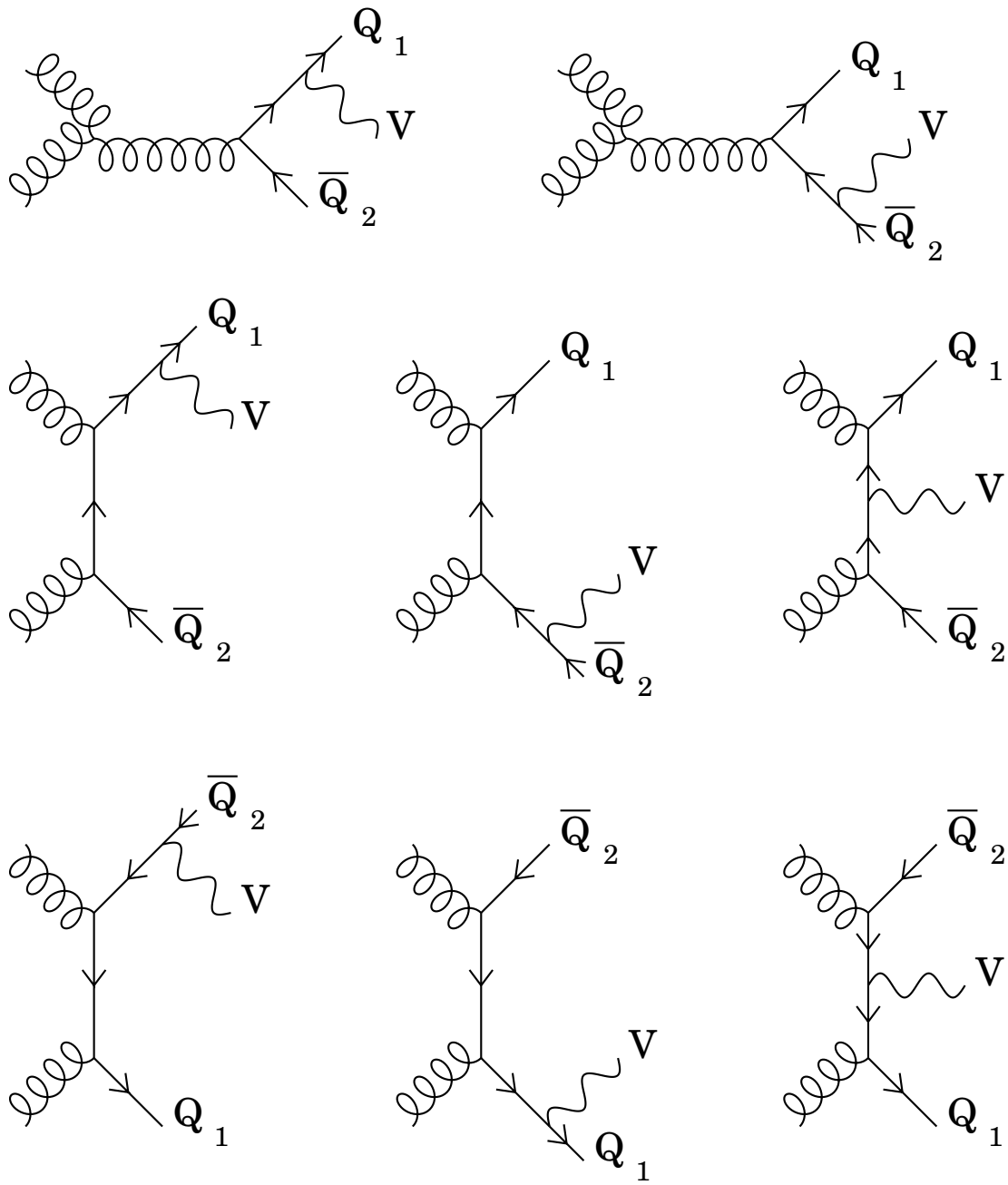


Fig. 6

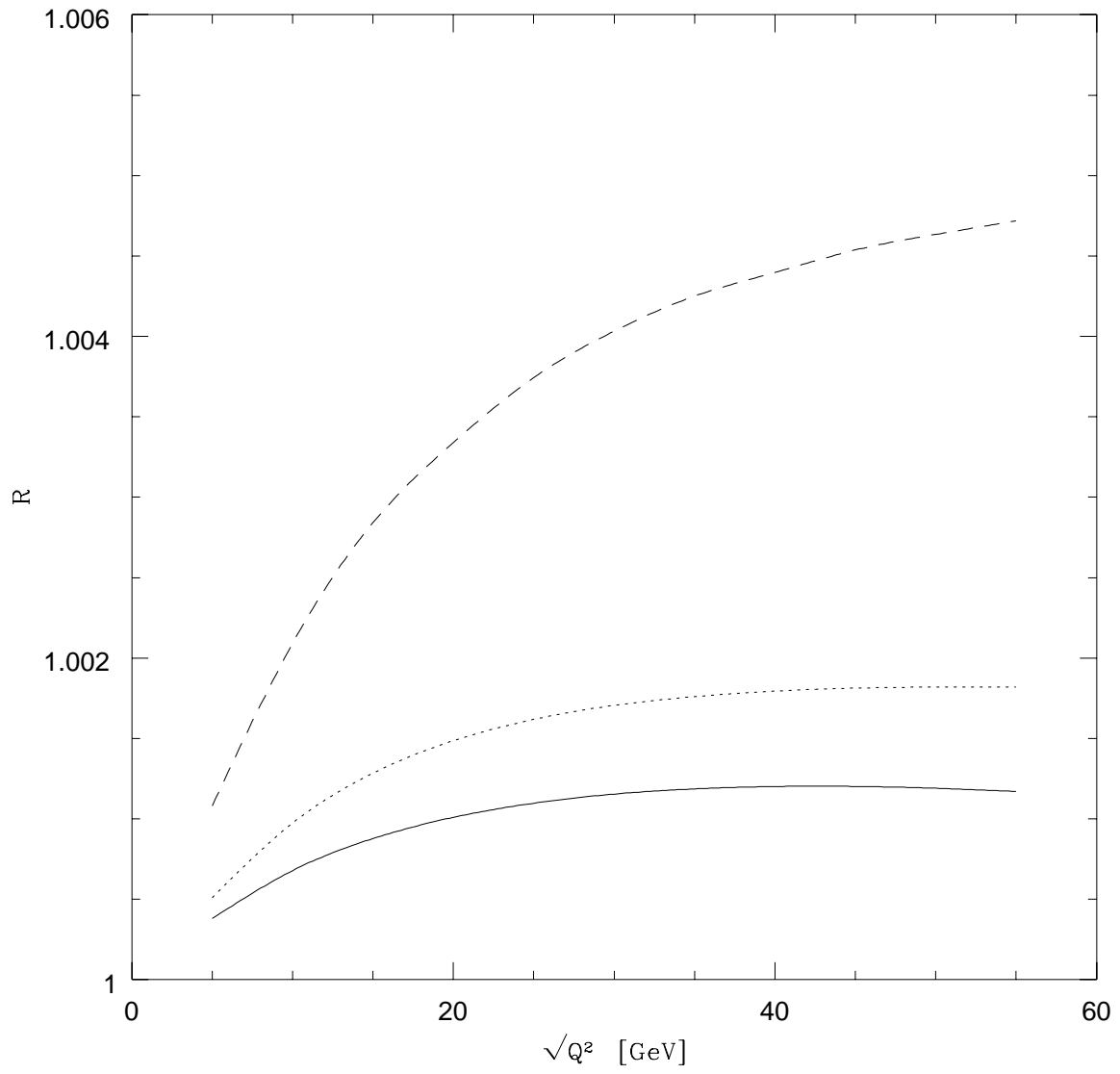


Fig. 7